Supplemental Information Inventory

Figures S1-9

Figure S1: Related to Figure 1.

Figure S2-5: Related to Figure 3.

Figure S6: Related to Figure 4.

Figure S7-9: Related to Figure 5.

Figures S10: Related to Figure 6.

Tables S1-8

Table S1. Genes constituting the protein–protein interaction (PPI) networks within identified modules, Related to Figure 3.

Table S2. Quality control parameters for single-cell transcriptomic datasets, Related to Figure 3.

Table S3. Subcluster composition and cell-cycle phase distribution of LDS10 and HDS10 cells, Related to Figure 3.

Table S4. IC_{50} values of LDS and HDS cells in response to DDP, ActD, and HHT treatment, Related to Figure 5.

Table S5 IC50 values (ng/mL) of HHT in LDS cells and HDS cells, along with the corresponding resistance indices (RI), related to Figure5.

Table S6 IC50 values (ng/mL) of HHT in LDS and HDS cells, along with the corresponding resistance indices (RI).

Table S7 Key parameters used for plasticity quantification across datasets, related to Figure 4 and Figure 6.

Supplemental Figures

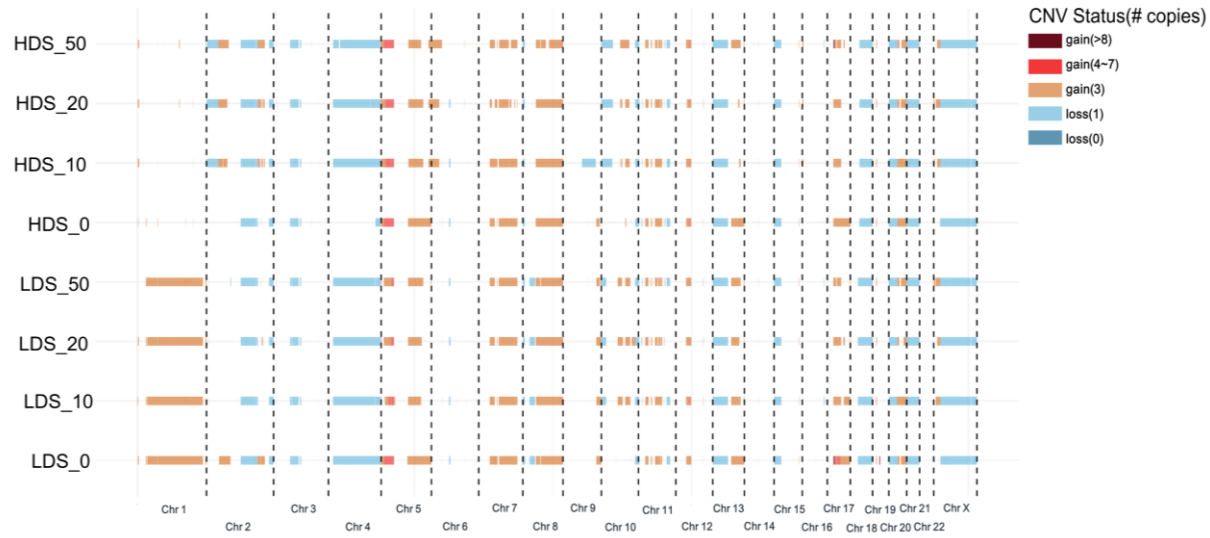


Figure S1. Copy number variation landscapes of LDS and HDS cells across passages 0 to 50.

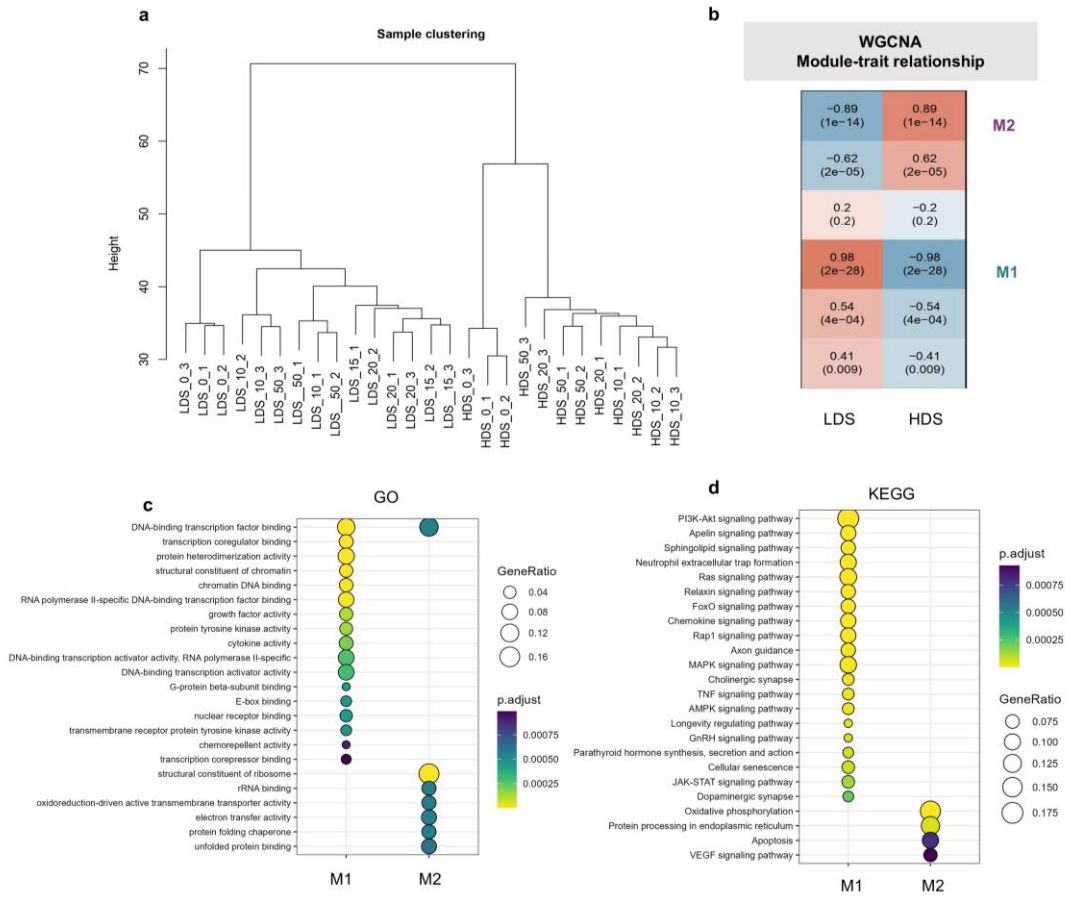


Figure S2. Gene co-expression network analysis across long-term experimental evolution.

a, Hierarchical clustering of transcriptomes from all samples used for weighted gene co-expression network analysis (WGCNA) to identify co-expression modules.

b, Correlation between module eigengenes and the HDS or HDS cell phenotypes. Module M1 showed the strongest positive correlation with the HDS phenotype, whereas module M2 was most strongly associated with the HDS phenotype.

c, Gene Ontology (GO) enrichment analysis of genes in modules M1 and M2.

d, Kyoto Encyclopedia of Genes and Genomes (KEGG) pathway enrichment analysis of genes in modules M1 and M2.



Figure S3. Chromatin accessibility landscapes of LDS and HDS cells across passages 0 to 50.

a, Specific-accessible chromatin peaks identified in LDS and HDS cells across passages 0 to 50.

b, Venn diagram summarizing transcription factors associated with significantly enriched motifs identified from differentially accessible regions.

c, Motifs specifically enriched in HDS cells and the biological functions of their corresponding transcription factors.

d, Motifs specifically enriched in HDS cells and the biological functions of their corresponding transcription factors.

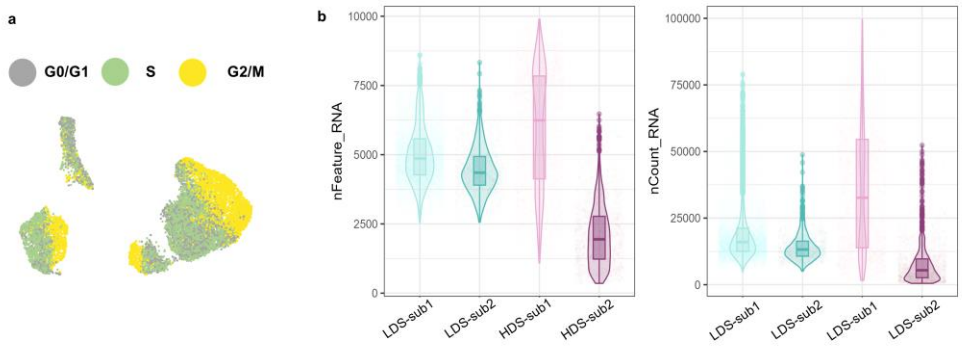


Figure S4. Cell cycle characteristics of LDS and HDS cell subclusters.

a, Cell cycle phase distribution of the identified subclusters, showing greater phase separation among HDS cell subclusters. The major LDS and HDS subclusters were not distinguished by differential expression of canonical cell cycle genes.

b, RNA feature statistics of LDS and HDS cell subclusters. HDS subclusters (HDS-sub1 and HDS-sub2) exhibited greater divergence in both *nFeature_RNA* and *nCount_RNA* distributions.

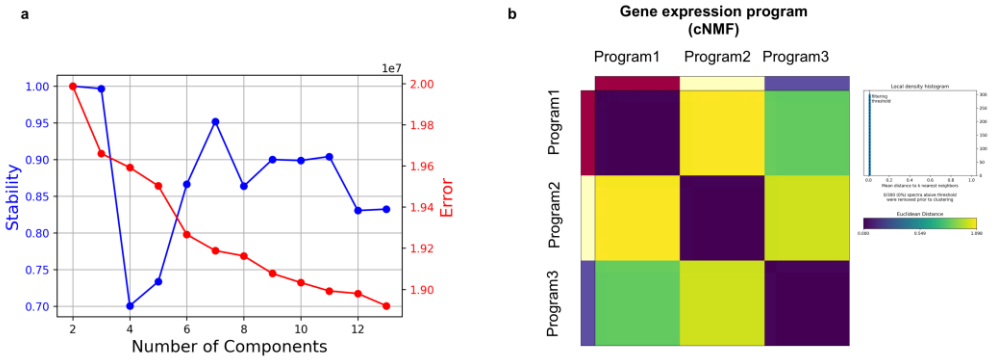


Figure S5. Identification of gene expression programs by consensus non-negative matrix factorization (cNMF).

a, Determination of the optimal factorization rank (*K*) for cNMF, indicating the highest stability at *K* = 3.

b, E-distances among the identified transcriptional programs.

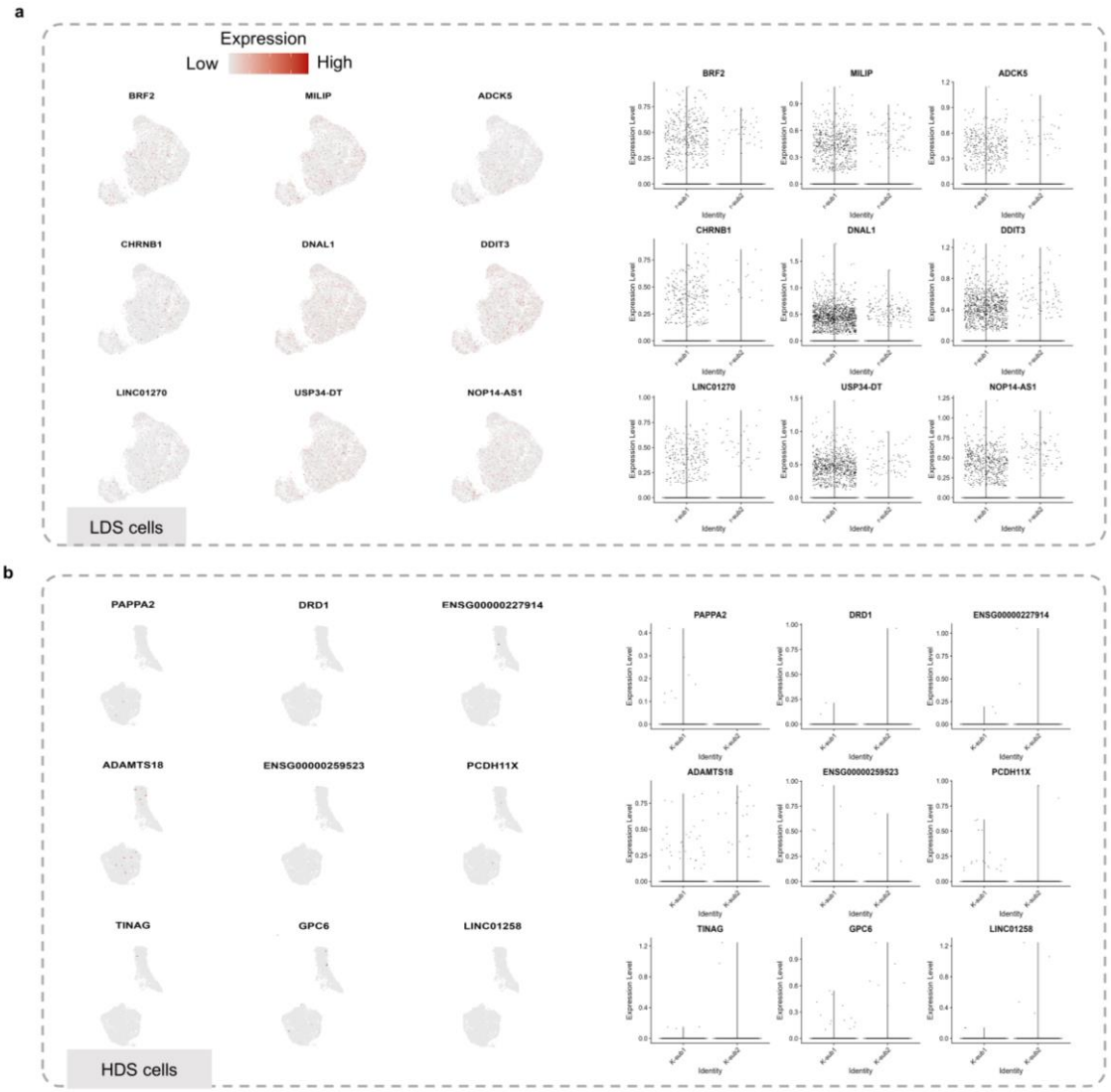


Figure S6. Highly plastic gene subnetworks in LDS and HDS cells.

a, Expression patterns of hub genes from the nine most plastic subnetworks in HDS cells.

b, Expression patterns of hub genes from the nine most plastic subnetworks in HDS cells.

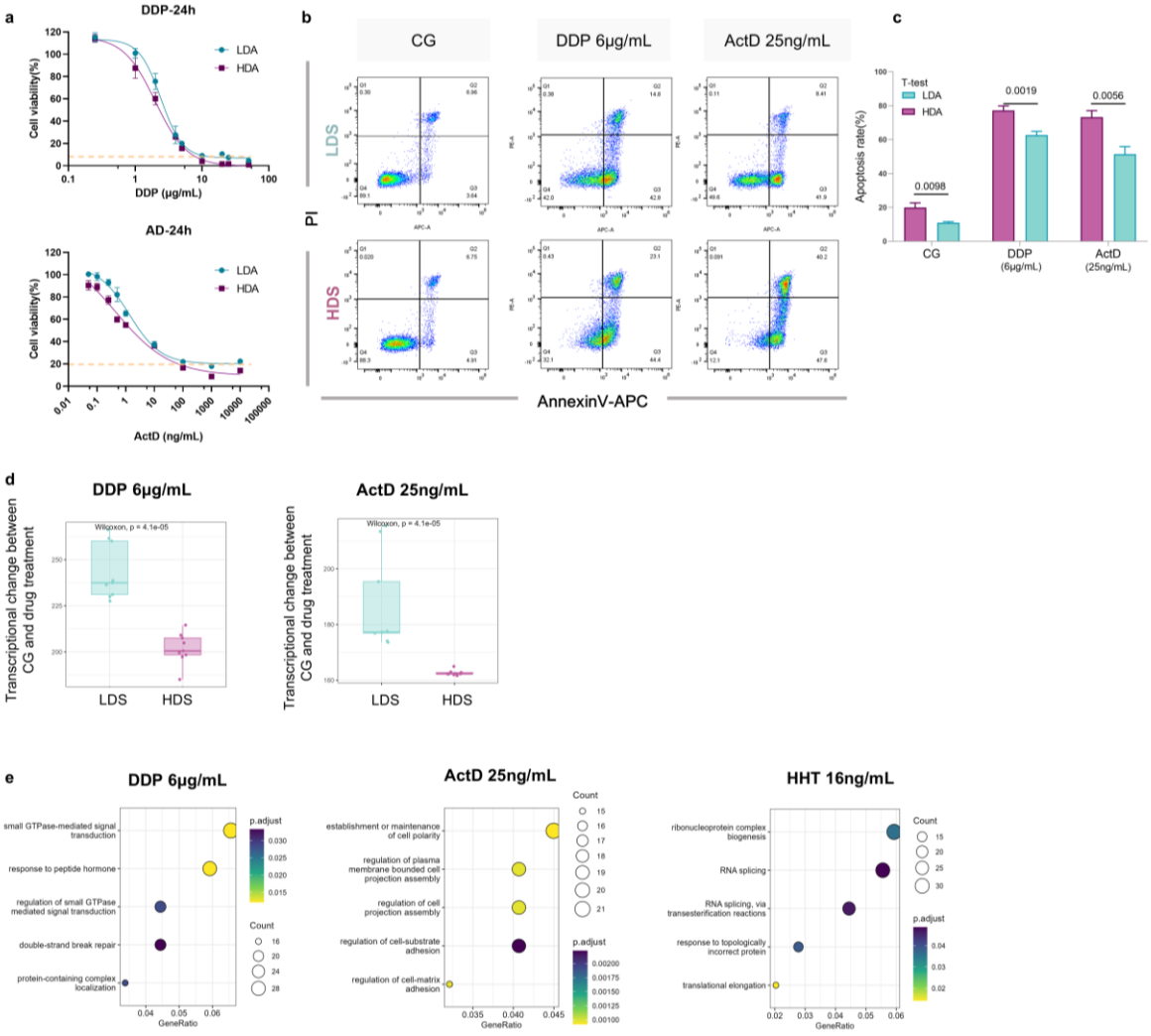


Figure S7. Responses of LDS and HDS cells to cisplatin (DDP) and actinomycin D (ActD).

a, Cell viability of LDS and HDS cells following 24 h treatment with cisplatin (DDP) or actinomycin D (ActD), measured using the CCK-8 assay.

b, Apoptosis of LDS and HDS cells following 24 h treatment with cisplatin or actinomycin D.

c, Quantification of apoptosis rates before and after drug treatment.

d, Transcriptomic changes in LDS and HDS cells before and after drug treatment.

e, Gene Ontology (GO) enrichment analysis of the major drug-induced transcriptional changes. The top 500 genes for DDP and ActD, or the top 600 genes for HHT, ranked by PC1 loadings from principal component analysis (PCA), were used for enrichment analysis.

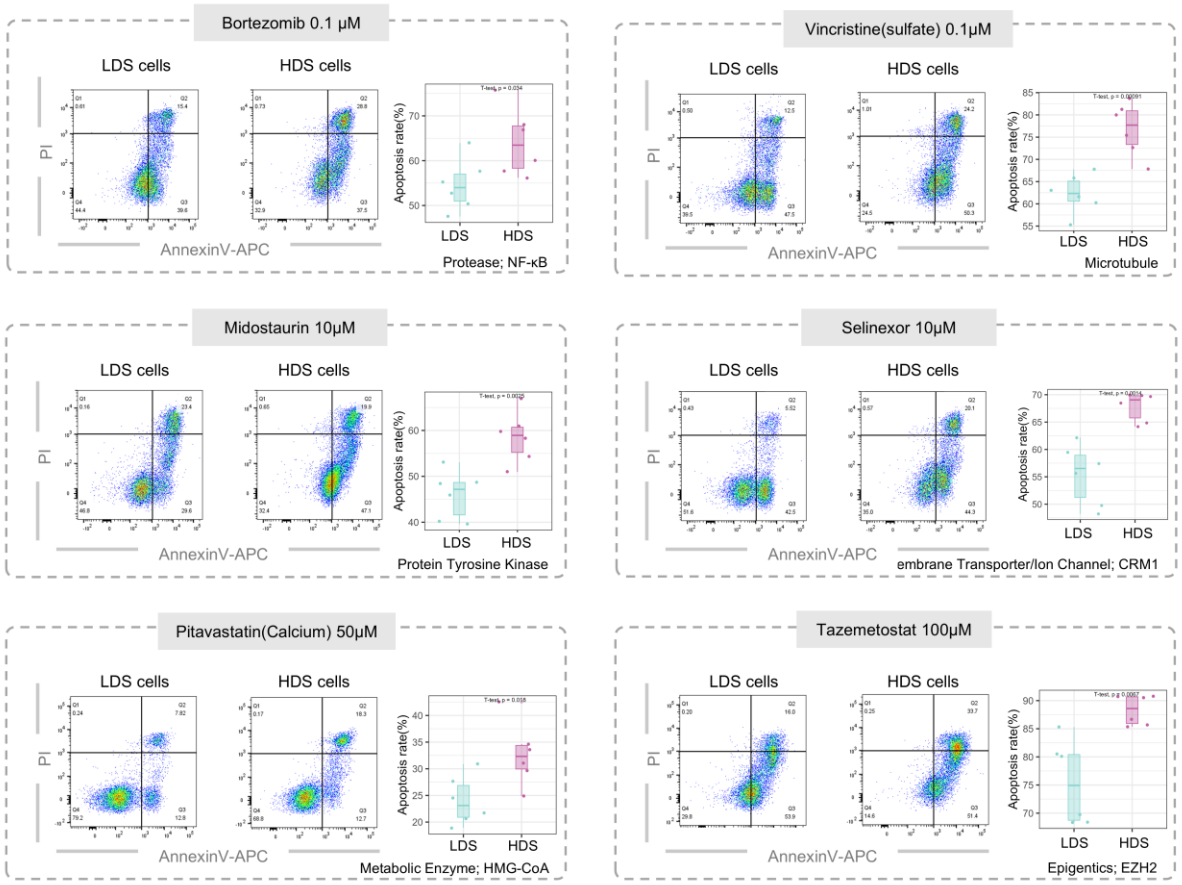


Figure S8. HDS cells exhibit broad-spectrum tolerance to multiple targeted therapies.

Apoptosis rates of LDS and HDS cells following treatment with six additional targeted agents affecting diverse cellular processes, including proteasome function, mitosis, tyrosine kinase signaling, ion transport, metabolism, and epigenetic regulation. *P* values were calculated using two-sided *t* tests.

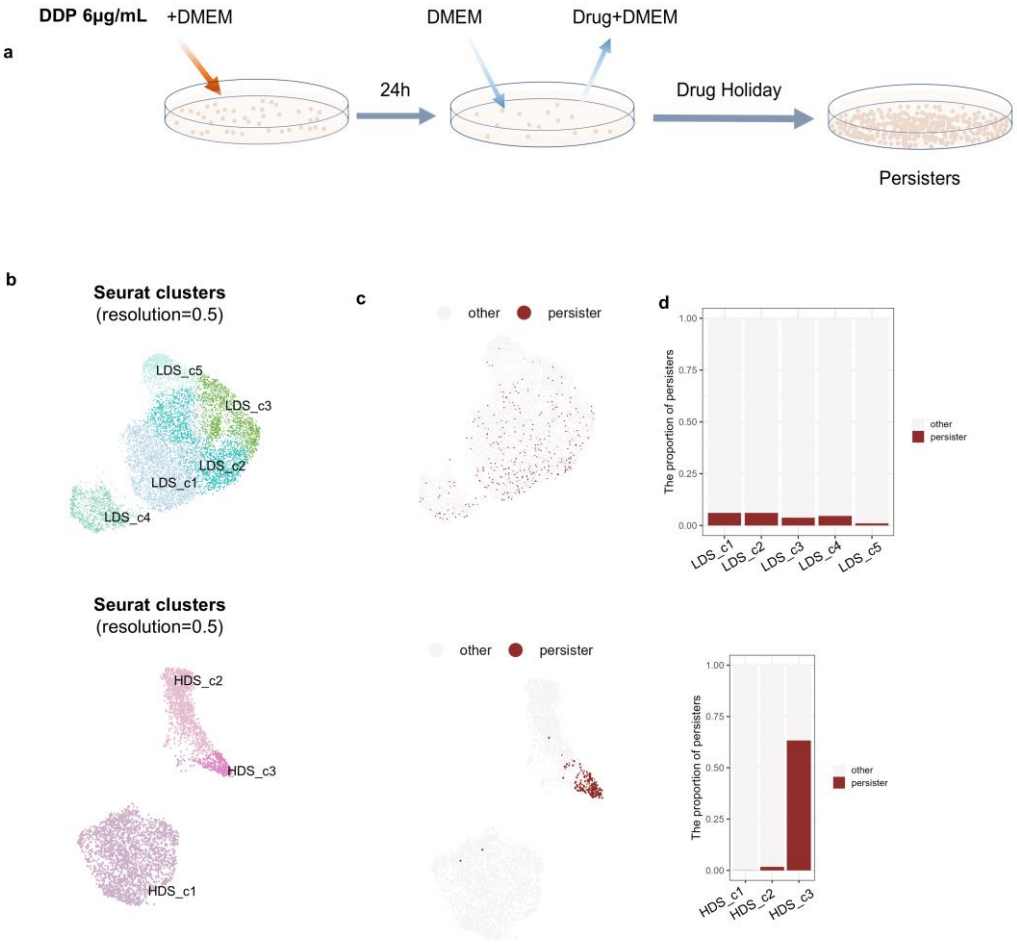


Figure S9. Inference of the origin of DDP persisters in LDS and HDS cells.

a, Schematic of the persister isolation strategy. Cells were treated with DDP for 48 h and subsequently recovered in drug-free medium until reaching approximately 70% confluence before transcriptomic profiling (*n* = 3).

b, High-resolution reclustering of single-cell transcriptomes from LDS and HDS cells (resolution = 0.5).

c, Identification of inferred persister cells within the original single-cell populations. A persister signature was defined using the top 500 upregulated genes, and the top 5% of cells based on signature scores were classified as inferred persisters.

d, Distribution of inferred persisters across LDS and HDS cell subclusters.

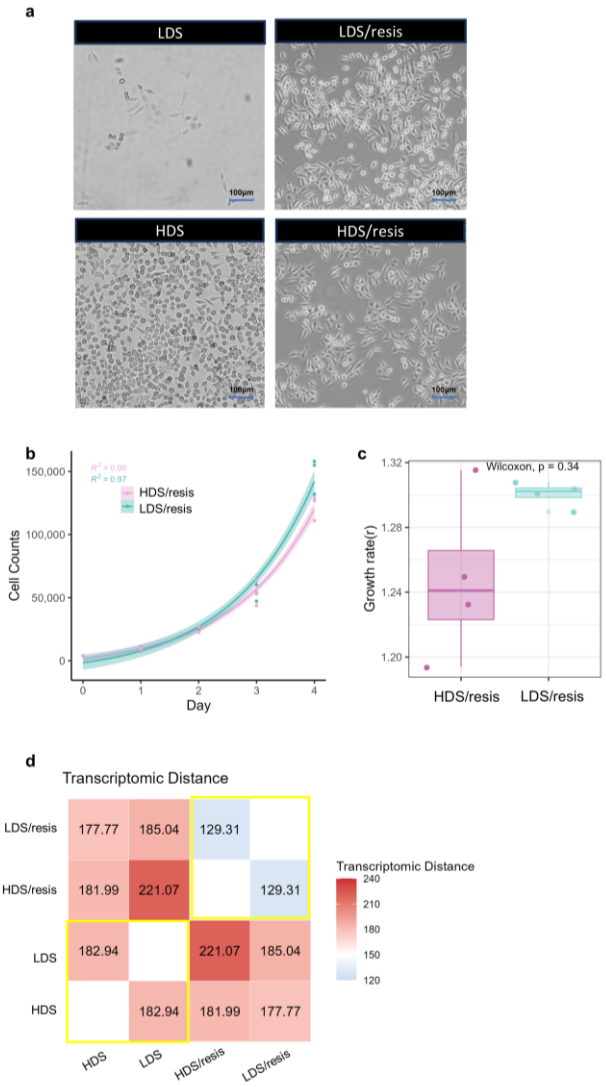


Figure S10. Phenotypic characterization of HHT-resistant LDS and HDS cells following long-term drug selection.

a, Representative cell morphology of LDS and HDS cells and their corresponding HHT-resistant derivatives (LDS/resis and HDS/resis) under bright-field microscopy (10×).

b, Logarithmic growth curves of LDS/resis and HDS/resis cells. Cells were seeded at 3,000 cells per well and counted daily for four consecutive days.

c, Comparison of growth rates during the logarithmic growth phase.

d, Transcriptomic divergence between parental LDS and HDS cells and their corresponding resistant derivatives, quantified using Euclidean distance.

Supplementary Tables

Table S1 Genes constituting the protein–protein interaction (PPI) networks within identified modules.

	Module genes in PPI
M1 (LDS-specific module)	LHX1, ACSL1, CRABP2, RARG, TLE4, ABCA1, AGER, SIGIRR, EDN2, ITK, TSC22D3, PLA2G4A, PDZD7, NRP2, SCN1B, SCNN1A, SYNJ2, CLDN3, CLDN15, NME1-NME2, ADCY7, AK4, BMF, CST3, TAOK3, IFI6, RPS6KA5, TRIM66, WHRN, ESPNL, LMO1, GABBR1, UNC5B, SUFU, GLI2, RASSF8, FBLN1, EFNA5, OCLN, LHX2, EBF1, PNPLA6, BCL2L11, CTSB, CTSO, BID, PTPRJ, SEMA4D, IFT140, WDR35, S1PR3, S1PR2, CD19, BAIAP2, DOCK1, TCF12, MAP1A, CREBRF, UCN, FSTL1, TNFRSF13C, KDM3A, SLC2A4, PDE3B, FADS2, ABLIM3, NRG1, GAB2, IQGAP2, BOC, LDB1, SSBP4, PTGS2, BBC3, JMY, RUNX3, LPIN1, TAF4B, RXRA, THRA, RUNX2, FGFR2, HSPG2, EGFR, NGEF, CRLF2, IL7, PLAAT3, PLD2, PTCH1, SMURF2, VIPR2, RAC3, PER1, CEBPA, PRKAB2, CBX6, CBX2, EZH1, SCML2, ENTPD2, PDE6G, SGPL1, CERS4, SGPP1, NR1D1, FOSL2, NR4A2, SNAI1, JUNB, EGR1, IL32, PRTN3, TLE1, HES1, GNG2, GNG4, GNG3, PLCB2, PREX1, PLCB4, GNB3, MYC, CCND2, CCND1, TLR3, UNC93B1, CAMK4, HDAC5, CCL26, CCL2, NOG, AMH, CD40, SRC, COL18A1, EDN1, MMP2, GADD45B, TP53, FOXO3, FOXO4, PER2, FOSB, HDAC4, SIRT1, PIK3CD, NGFR, CDYL2, PHLPP2, AFAP1, CD83, PFKFB2, VEGFC, SEMA3B, COL15A1, F11R, MAP3K2, SGK1, LPAR1, ADGRG1, PPP4R2, INO80C, TAF7, TRIO, VAV3, PLXNA2, MAP2K3, H2BC7, H2BC4, H2AC8, ANGPTL4, RUNX1, DNAJC3, HSP90B1, IRF7, IL15RA, TLR6, BMPER, BMP6, TLR4, IL18, ABLIM1, DOCK5, AREG, ERRFI1, PDGFC, EPS8, NRG4, NEDD4, PIK3C2B, UBASH3B, IFI16, AKT3, SETD7, KLF4, SQSTM1, LPL, NDUFS6, MGLL, PPP2R2A, PPP2R3A, NRIP1, CREB3, FGFBP1, PTX3, BMP2, MET, EPHA2, EPHA5, EPHA7, IL15, EPAS1, CDS1, LPCAT1, GLP2R, H2AC11, H2AJ, H2AC15, RRM2B, LIFR, FGF2, LIF, SPHK1, NPAS2, CDH2, NAB1, MLLT3, AFF1, ELL2, H3-5, H3C1, H4C9, H4C3, H3C8, H4C8, ASF1A, GNG13, GNGT1, CDKN1A, CDKN2B, IL6, NFKB2, NFKBIE, RELB, TIMP4, PPARGC1A, PPARG
M2 (HDS specific module)	TBC1D5, MPV17, CRTC2, CRTC1, YEATS2, GABARAP, ARRB2, NR4A1, CREB3L1, MKNK2, WASF1, SPATA13, RAC2, RPL12, HSPB1, CTTNBP2NL, MAPK3, ULK1, TRIB3, NACA2, SUCLA2, HIBCH, CSNK2B, MB, BAK1, ENDOG, POLE4, GABARAPL1, CCPG1, MALSU1, MRM3, POLG, SLC25A4, RPL34, RPLP1, RPL36A, RPL22L1, LRRC47, AURKAIP1, MRPS28, BAD, TBC1D7, ATP1B3, EIF2S1, HSPA1L, DNAJB1, MRPL47, MRPL23, MRPL39, MRPL34, NDUFC1, NDUFAB1, NDUFA11, NDUFS3, UQCRFS1, NDUFAF4, NDUFA2, CYCS, HSPB8, ATP5MG, ATP5ME, UQCR10, ATP5F1E, SSR3, RPL9, HSPA5, OSTC, SEC61A1, EMG1, RRP7A, RPS28, NOP9, RPS10, BYSL, DDIT3, MAPK14, CCT2, PPP2CB, RPS3, GTF2A2, TAF13, MRPL12, MRPL20, POLR2C

Table S2 Quality control parameters for single-cell transcriptomic datasets.

Quality control Step	**LDS 10**	**HDS 10**	**Description**
Gene count (nFeature_RNA)	<10000	2500–10000	Remove low-quality cells and potential multiplets
UMI count (nCount_RNA)	<100000	<80000	Remove cells with abnormally high expression
Mitochondrial % (mt_percent)	1–6%	<12%	Remove cells with high mitochondrial content
decontX contamination cutoff	<0.75	<0.7	Remove cells with high ambient RNA contamination
DoubletFinder pN	0.25	0.25	Parameter for doublet detection
Cell count after quality control	3665	8202	

Table S3 Subcluster composition and cell-cycle phase distribution of LDS10 and HDS10 cells.

Sample	**Subcluster**	**Proportion of cells (%)**	**G1 (%)**	**S (%)**	**G2/M (%)**	**χ^2**	**p-value**
LDS 10	LDS-sub1	88.81	20.96	39.46	39.58	14.86	0.0005927
LDS 10	LDS-sub2	11.19	25.38	33.66	40.96		
HDS 10	HDS -sub1	62.43	16.22	50.47	16.78	459.2	< 0.0001
HDS 10	HDS -sub2	37.57	72.00	7.52	39.51		

Table S4 IC_{50} values of LDS and HDS cells in response to DDP, ActD, and HHT treatment.

	DDP(μg/mL)	**ActD (ng/mL)**	**HHT (ng/mL)**
LDS cell	2.422	1.297	3.435
HDS cell	1.996	0.4116	5.092

Table S5 IC50 values (ng/mL) of HHT in LDS cells and HDS cells, along with the corresponding resistance indices (RI).

	Sensitive	**Resistance**	**RI**
LDS cell	3.345	19.43	5.809
HDS cell	5.092	24.95	4.900

Table S6 Sources and detailed descriptions of public datasets used in this study.

Public data	**Database-id**	**Source (DOI)**	**Description**	**Platform**
dataset 1	CNGBdb-CNP0004330	10.1038/s41467-023-43991-9	42 cell lines with single-cell transcriptome data, including two non-tumor cell lines.	10×
dataset 2	BioProject-PRJNA591860	10.1038/s41467-020-17440-w	Single-cell transcriptome data from lung cancer clinical samples collected before, during, and after treatment.	384-well plate–based Smart-seq2
dataset 3	GEO-GSE222596	10.1038/s41467-024-51424-4	Single-cell transcriptome data from the SUM59PT cell line treated with Paclitaxel (50 nM) for 2 days, followed by recovery under normal culture conditions for 15 days.	Multi-seq

Table S7 Key parameters used for plasticity quantification across datasets.

data	***P* (top variable genes)**	**corr_threshold**	**k**
LDS/HDS	2000	0.05	50
dataset 1	8000	0.3	30
dataset 2	2000	0.4	50
dataset 3	2000	0.1	50